Behavior Research Methods
https://doi.org/10.3758/s13428-023-02197-z

Measuring the nonselective effects of motor inhibition using isometric force recordings

Benjamin O. Rangel[1,2,3] · **Giacomo Novembre**[4] · **Jan R. Wessel**[2,5,6]

Accepted: 10 July 2023

Abstract
Inhibition is a key cognitive control mechanism humans use to enable goal-directed behavior. When rapidly exerted, inhibitory control has broad, nonselective motor effects, typically demonstrated using corticospinal excitability measurements (CSE) elicited by transcranial magnetic stimulation (TMS). For example, during rapid action-stopping, CSE is suppressed at both stopped and task-unrelated muscles. While such TMS-based CSE measurements have provided crucial insights into the fronto-basal ganglia circuitry underlying inhibitory control, they have several downsides. TMS is contraindicated in many populations (e.g., epilepsy or deep-brain stimulation patients), has limited temporal resolution, produces distracting auditory and haptic stimulation, is difficult to combine with other imaging methods, and necessitates expensive, immobile equipment. Here, we attempted to measure the nonselective motor effects of inhibitory control using a method unaffected by these shortcomings. Thirty male and female human participants exerted isometric force on a high-precision handheld force transducer while performing a foot-response stop-signal task. Indeed, when foot movements were successfully stopped, force output at the task-irrelevant hand was suppressed as well. Moreover, this nonselective reduction of isometric force was highly correlated with stop-signal performance and showed frequency dynamics similar to established inhibitory signatures typically found in neural and muscle recordings. Together, these findings demonstrate that isometric force recordings can reliably capture the nonselective effects of motor inhibition, opening the door to many applications that are hard or impossible to realize with TMS.

Keywords TMS · Isometric Force · Beta · Stop-Signal · SSRT · Inhibitory Control · Motor Control · CVF

Introduction

Stopping actions is almost as essential as starting them. Inhibitory control must be rapidly implementable to avoid potential threats. A fronto-basal ganglia (FBg) network implements such rapid inhibition following salient signals (Aron & Poldrack, 2006; Erika-Florence et al., 2014; Wager et al., 2005; Wessel & Aron, 2017). Frontal cortical areas quickly activate the subthalamic nucleus (STN) of the basal ganglia via a hyper-direct fiber pathway, ultimately suppressing thalamocortical output (Chen et al., 2020; Miocinovic et al., 2018; Nambu et al., 2002; Wessel & Aron, 2017). Notably, when inhibition is exerted via this route, it has broad, nonselective effects on the motor system, typically demonstrated using corticospinal excitability (CSE). CSE can be measured by combining transcranial magnetic stimulation (TMS) and electromyography to elicit a motor-evoked potential, which indexes the net excitability of the corticospinal tracts underlying specific muscles (Bestmann & Duque, 2016; Lazzaro & Rothwell, 2014; Volz et al., 2015). When humans stop an action, the CSE of the involved muscles is suppressed (Coxon et al., 2006; Leocani et al., 2000). Notably, this suppression extends even to effectors uninvolved in the movement (Badry et al., 2009)—an effect that is specifically attributable to the STN (Wessel et al., 2022).

Significance statement

Inhibitory control allows humans to override inappropriate actions during goal-directed behavior. When inhibition is rapidly exerted on the motor system, it has broad, nonselective effects. For example, when a foot movement is rapidly stopped, other task-unrelated muscles also show signs of inhibition. This is typically shown using transcranial magnetic stimulation (TMS) of the motor cortex. However, TMS is contraindicated in many populations of interest, produces artifacts in neural recordings, is distracting to the subject, and has very limited time resolution. Here, we demonstrate clear nonselective effects of inhibitory control using isometric force recordings from a task-unrelated muscle during a stop-signal task. This simple method has high time resolution, no contraindications, and could be readily combined with other imaging methods.

Extended author information available on the last page of the article

Published online: 07 August 2023

TMS-based CSE measurements of these broad, nonselective effects of inhibitory control have implicated the FBg-STN network across many control-demanding scenarios. For example, unexpected stimuli (Dutra et al., 2018; Tatz et al., 2021), action errors (Guan & Wessel, 2022), and response conflict (Wessel et al., 2019) are all followed by nonselective CSE suppression—and indeed, all activate the STN (Cavanagh et al., 2014; Frank et al., 2007; Herz et al., 2017; Siegert et al., 2014; Wessel et al., 2016). Furthermore, TMS-based CSE measurements have been used to study response preparation (Bestmann & Duque, 2016; Leocani et al., 2000; Raud et al., 2020), interhemispheric interactions (Fiori et al., 2017; Hamada et al., 2014; Hannah & Rothwell, 2017), and motor pathologies (Badawy et al., 2013; Chowdhury et al., 2018; Jahanshahi & Rothwell, 2017; Smith & Stinear, 2016).

However, the TMS-based CSE method has multiple substantial downsides. First, TMS is contraindicated in several populations, including patients with epilepsy, implanted neurostimulators, or metallic skull implants (Rossi et al., 2020). Notably, this includes virtually all populations in which intracranial recordings are performed, which would allow the highest-fidelity insights into FBg-STN neurophysiology. Second, TMS-based CSE has poor temporal resolution, due to both the recharging of TMS stimulators, which rate-limits CSE measurements to ~1 Hz (Hallett & Chokroverty, 2006), and the habituation effects of repeated TMS on CSE itself (Fitzgerald et al., 2006). Third, TMS introduces tactile and auditory stimulation, which can interfere with behavior. Fourth, the magnetic field produced by TMS makes it challenging to combine with other imaging methods (Ilmoniemi et al., 2015; Rogasch et al., 2017). Finally, TMS stimulators are expensive and space-consuming.

Here, we aimed to test an alternative method to quantify the nonselective effects of inhibitory motor control—ideally, one that addresses the shortcomings of TMS-based CSE measurements. We hypothesized that nonselective inhibitory effects on the motor system may be found in the modulation of isometric force. This was motivated by several recent observations. First, unexpected perceptual events evoke a multiphasic stimulus-locked modulation of isometric force (Novembre et al., 2018, 2019), starting with a short-latency force reduction that is reminiscent of the fast CSE suppression observed after such events (Dutra et al., 2018; Tatz et al., 2021). Moreover, this complex modulation of force was coupled with modulations of scalp-electroencephalography (EEG) activity, including a fronto-central positivity with morphology similar to the stop-signal P3 (De Jong et al., 1990; Kok et al., 2004; Wessel & Aron, 2015). Second, unexpected events modulate beta-like oscillatory activity (~20 Hz) in isometric force recordings, coupled with isofrequent EEG beta activity originating from the primary motor and premotor cortices contralateral to the limb used to exert force (Novembre et al., 2019). This result should be highlighted given that cortical beta activity is also found during action-stopping (N. Swann et al., 2009; Wagner et al., 2018; Wessel, 2020). In view of these similarities, recent theoretical work has suggested exploring action-stopping using force recordings such as those described above (Novembre & Iannetti, 2021).

Thirty participants performed the stop-signal task (SST; (Logan et al., 1984) using foot pedals. Successful stopping of foot responses leads to CSE suppression at the task-unrelated hand (Tatz et al., 2021). Here, participants instead exerted steady isometric pressure on a force transducer using the fingers of the task-unrelated hand. Our primary hypothesis was that isometric finger-force output would be transiently reduced when participants successfully stopped their foot responses, indicating nonselective inhibition. After indeed finding this outcome, we correlated the magnitude of this effect to stop-signal reaction time. Finally, we explored both the frequency dynamics of the isometric force trace (Novembre et al., 2019) and its coefficient of variation (Davis et al., 2020; Hyngstrom et al., 2014).

TMS-based CSE measurements of these broad, nonselective effects of inhibitory control have implicated the FBg-STN network across many control-demanding scenarios. For example, unexpected stimuli (Dutra et al., 2018; Tatz et al., 2021), action errors (Guan & Wessel, 2022), and response conflict (Wessel et al., 2019) are all followed by nonselective CSE suppression—and indeed, all activate the STN (Cavanagh et al., 2014; Frank et al., 2007; Herz et al., 2017; Siegert et al., 2014; Wessel et al., 2016). Furthermore, TMS-based CSE measurements have been used to study response preparation (Bestmann & Duque, 2016; Leocani et al., 2000; Raud et al., 2020), interhemispheric interactions (Fiori et al., 2017; Hamada et al., 2014; Hannah & Rothwell, 2017), and motor pathologies (Badawy et al., 2013; Chowdhury et al., 2018; Jahanshahi & Rothwell, 2017; Smith & Stinear, 2016).

However, the TMS-based CSE method has multiple substantial downsides. First, TMS is contraindicated in several populations, including patients with epilepsy, implanted neurostimulators, or metallic skull implants (Rossi et al., 2020). Notably, this includes virtually all populations in which intracranial recordings are performed, which would allow the highest-fidelity insights into FBg-STN neurophysiology. Second, TMS-based CSE has poor temporal resolution, due to both the recharging of TMS stimulators, which rate-limits CSE measurements to ~1 Hz (Hallett & Chokroverty, 2006), and the habituation effects of repeated TMS on CSE itself (Fitzgerald et al., 2006). Third, TMS introduces tactile and auditory stimulation, which can interfere with behavior. Fourth, the magnetic field produced by TMS makes it challenging to combine with other imaging methods (Ilmoniemi et al., 2015; Rogasch et al., 2017). Finally, TMS stimulators are expensive and space-consuming.

Here, we aimed to test an alternative method to quantify the nonselective effects of inhibitory motor control—ideally, one that addresses the shortcomings of TMS-based CSE measurements. We hypothesized that nonselective inhibitory effects on the motor system may be found in the modulation of isometric force. This was motivated by several recent observations. First, unexpected perceptual events evoke a multiphasic stimulus-locked modulation of isometric force (Novembre et al., 2018, 2019), starting with a short-latency force reduction that is reminiscent of the fast CSE suppression observed after such events (Dutra et al., 2018; Tatz et al., 2021). Moreover, this complex modulation of force was coupled with modulations of scalp-electroencephalography (EEG) activity, including a fronto-central positivity with morphology similar to the stop-signal P3 (De Jong et al., 1990; Kok et al., 2004; Wessel & Aron, 2015). Second, unexpected events modulate beta-like oscillatory activity (~20 Hz) in isometric force recordings, coupled with isofrequent EEG beta activity originating from the primary motor and premotor cortices contralateral to the limb used to exert force (Novembre et al., 2019). This result should be highlighted given that cortical beta activity is also found during action-stopping (N. Swann et al., 2009; Wagner et al., 2018; Wessel, 2020). In view of these similarities, recent theoretical work has suggested exploring action-stopping using force recordings such as those described above (Novembre & Iannetti, 2021).

Thirty participants performed the stop-signal task (SST; (Logan et al., 1984) using foot pedals. Successful stopping of foot responses leads to CSE suppression at the task-unrelated hand (Tatz et al., 2021). Here, participants instead exerted steady isometric pressure on a force transducer using the fingers of the task-unrelated hand. Our primary hypothesis was that isometric finger-force output would be transiently reduced when participants successfully stopped their foot responses, indicating nonselective inhibition. After indeed finding this outcome, we correlated the magnitude of this effect to stop-signal reaction time. Finally, we explored both the frequency dynamics of the isometric force trace (Novembre et al., 2019) and its coefficient of variation (Davis et al., 2020; Hyngstrom et al., 2014).

Methods

Participants

Thirty-three adult human participants were recruited for this study. Two datasets were incomplete due to hardware errors, and the data for one additional participant were rejected for violation of the race model (see "Behavioral analysis"). This led to a final sample of 30 participants (age mean ± SD = 18.8 ± 1.6, 19 female, 29 right-handed). Participants were paid $15 per hour or received course credit for their participation in the study. All participants had normal or corrected-to-normal vision. The experiment was approved by the ethics committee at the University of Iowa (IRB #201511709).

Experimental task and procedure

Stimuli were presented via an Ubuntu Linux computer, running Psychtoolbox-3 (Brainard, 1997) in MATLAB 2017a (The MathWorks, Natick, MA, USA). Participants sat upright with their arms resting on a supportive platform placed on the armrests of the chair. Participants responded to stimuli during the task using left and right foot pedals (Kinesis Savant Elite 2), where they performed a version of the classic stop-signal task (Logan et al., 1984) while attempting to maintain a constant pinch-grip force with their right hand (Fig. 1). Stop-signal task stimuli were presented on an all-gray background. All trials began with a black fixation cross (500 ms), followed by a black arrow (1000 ms) pointing left or right (go signal). Participants were instructed to respond to the go signal using foot pedals (left pedal for left-facing arrows, and right pedal for right-facing arrows) using both feet, within the 1000 ms that the arrow was displayed. The arrow would immediately disappear following a response. The go signal was followed by a variable-length intertrial interval (ITI) which ensured that all trials had a total length of 3 s. If participants responded to the go signal, a black fixation cross was displayed during the ITI; if they did not respond, the message "TOO SLOW" was displayed in red text instead. During one third of the trials, the go signal was followed by a stop signal (i.e., the black arrow turning red) after a stop-signal delay (SSD). Participants were instructed to withhold their response on these trials. The SSD began at 200 ms and was subsequently adjusted in steps of 50 ms (added to the SSD after successful stop trials and subtracted after failed stop trials) with the goal of participants successfully stopping their responses on half of all stop trials (Verbruggen et al., 2019). Participants performed 10 blocks, each of 60 trials. At the end of each block, performance feedback was displayed on the screen. Participants were instructed that responding quickly on Go trials and stopping successfully on Stop trials were equally important. Visual stop signals are not considered startling stimuli, and this was further confirmed by comparing the resulting force traces from our study (Fig. 3A) with previous work (Novembre et al., 2018).

Force recording

Participants held the force transducer between their right index finger and thumb throughout the blocks of the task.

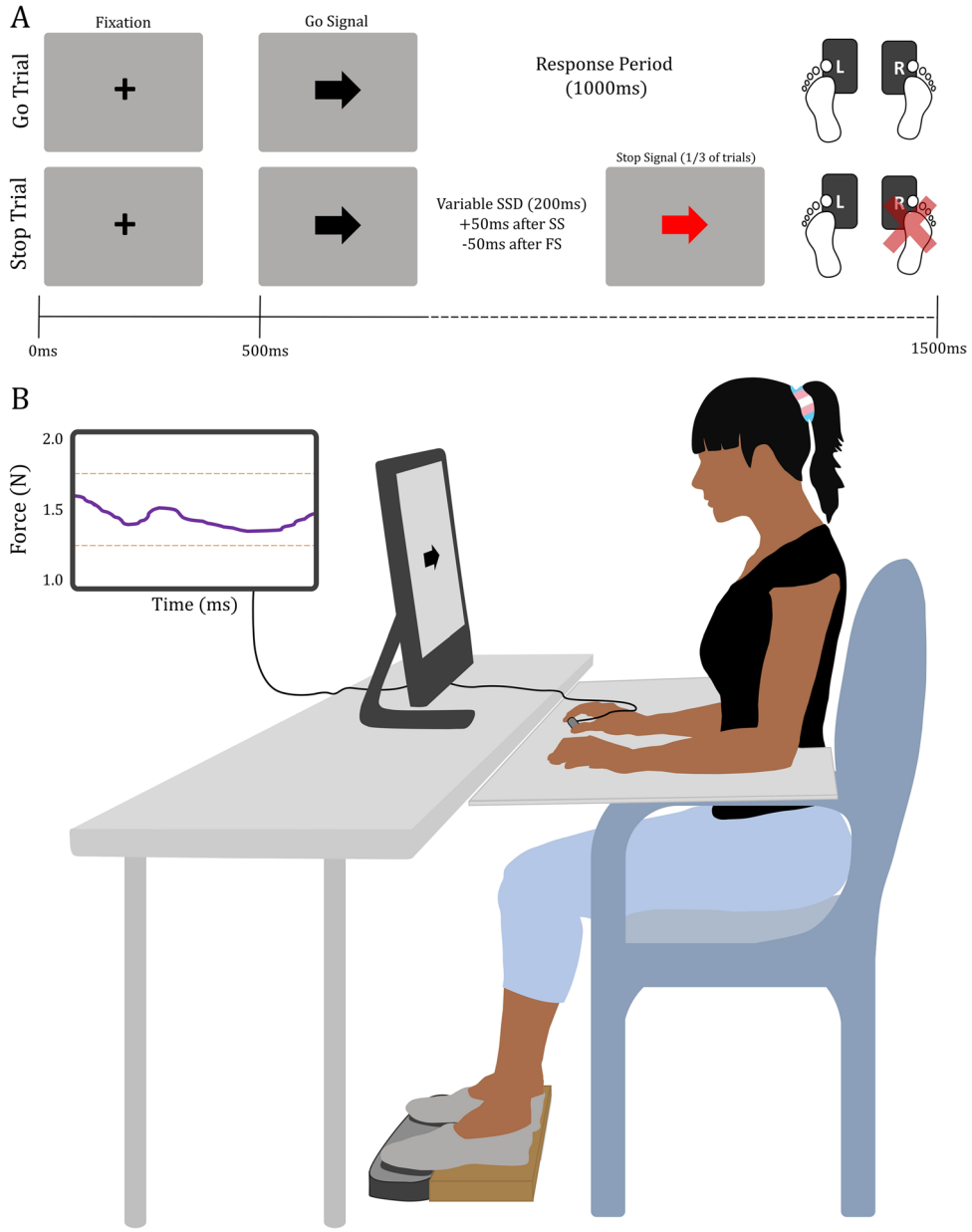

Fig. 1 Paradigm and task diagram. *Note.* Subjects performed a stop-signal task while attempting to maintain a constant isometric force. **A** During both stop and go trials (2/3 of trials), the fixation cross was presented for 500 ms, before the onset of the go signal (black arrow). Subjects then had 1000 ms to respond, using the foot pedals. During stop trials, the go signal was followed by the stop signal (red arrow) following a variable SSD, beginning at 200 ms (+50 ms after successful stop, −50 ms after failed stop). **B** All subjects held the force transducer in their right hand, between their index finger and thumb. Their arms were supported on a wooden platform, which rested on the chair arms. A wooden board was placed under the subject's feet to elevate their toes above the foot pedals and prevent fatigue. Live force recordings were presented on a second computer screen, which was outside the subjects' direct view. Prior to each block, subjects would direct their view towards the second screen to recenter their force output ~1.5 N

Live force data were recorded using a highly sensitive force/torque sensor (Nano17, ATI Industrial Automation, Rochester Hills, MI, USA), with custom 3D-printed finger grips attached to the sensor. The live force data were recorded and displayed via a separate Windows 7 computer running MATLAB 2020b, using custom scripts. Force was recorded at a rate of 3000 Hz and then resampled to a rate of 1000 Hz for display purposes. The monitor showing the force data was placed on a shelf out of direct view of the participants, except for the calibration time periods between blocks. A twist-tie secured the bottom transducer grip to their thumb, and they rested their forearm and hand on the supportive platform placed on the armrests of the chair. Prior to the beginning of each task block, participants were instructed

to direct their gaze towards the second screen displaying the live force readings. They were instructed to stabilize their force output within a range of 1.25–1.75 N (Fig. 1B). This target range was chosen based on previous work (Novembre et al., 2018) and was the same for all participants. Once they felt that they were steady enough, the participants would look back towards the task screen, and the experimenter would start the task block. Participants wore a sun visor to obscure any peripheral view of the second screen when performing the task.

Electromyography (EMG) recording

EMG was recorded from the left and right soleus muscles of each participant. The two recording electrodes (Kendall™ 530 Series, ref 31013926) were adhered vertically adjacent to each other, along the midline of the soleus muscles directly below the gastrocnemius, while the ground electrode was placed on the medial malleolus of the tibia. Each set of electrodes were connected to a Grass P511 amplifier (Grass Products, West Warwick, RI, USA; 2000 Hz sampling rate, filters: 30 Hz high-pass, 1000 Hz low-pass, 60 Hz notch). A CED Micro 1401-3 sampler (Cambridge Electronic Design Ltd., Cambridge, UK) triggered a 1500 ms EMG sweep, 500 ms before the go signal on each trial. Sweeps were recorded using CED Signal software (version 6).

Behavioral analysis

Behavioral data were processed following consensus protocols for analysis of the stop-signal task (Verbruggen et al., 2019). Trials with incorrect responses, missing responses on Go trials, or responses faster than 150 ms, or where the foot pedal was prematurely depressed were rejected (0.64% of trials [0–2.5%]). Blocks where the proportion of successful stops fell below .25 or exceeded .75 were also rejected (this was the case for 1 block out of 10 in $n = 3$, 2 blocks in $n = 1$, and 3 blocks in $n = 1$). Participants' stop-signal reaction time (SSRT) was then calculated using the integration method (Matzke et al., 2018).

Force data analysis

Single-subject raw data were bandpass-filtered (0.1–40 Hz) before being epoched relative to the arrow onset (−500 to 2500 ms). Any trial rejected during the behavioral analysis was removed from the force analysis as well. The remaining trials were baseline-corrected to the −250 to 0 ms pre-arrow period. Trial epochs were screened for outliers within the −250 to 850 ms time window. Specifically, trials with large fluctuations in force (outside −0.3 to 0.3 N) were removed (0.54% of trials [0–3%]). Then, the remaining trials were screened for force fluctuations outside 4 SDs of the mean of all trials, regardless of condition (4.0% of trials [2–6.2%], cf. Novembre et al., 2019). The mean percentage of trials rejected for subjects was 8.0% [2–19.3%] for subjects without block rejections. The rejection percentages are listed in Table 1. Participant data were then averaged by condition. In a separate analysis, we epoched force data relative to the response (−1500 to 1500 ms). These trials were baseline-corrected to the −1500 ms to −750 ms pre-response period. Further processing was performed as described above.

Time-frequency analysis of the force trace

Continuous force data were bandpass-filtered (0.1–50 Hz) before being convolved with a complex Morlet wavelet (3–10 cycles) for 50 frequencies (1–50 Hz; Cohen 2014). Power was estimated using the squared magnitude of the complex wavelet-convolved data. Time-frequency power estimates were then epoched relative to the arrow and response (same time span as in the force data). Trials marked as behavioral rejections and outliers identified during the force data analysis were removed. Baseline correction (decibel conversion) was performed per condition (−500 to −200 ms pre-arrow) before averaging.

For our control analysis on the time-frequency data, the same wavelet parameters were used as above. Prior to decomposition, the average force trace for each condition (Go, successful stop [SS], failed stop [FS]) and for each subject was subtracted from the continuous data, time-locked to the arrow onset. Following decomposition, the same baseline correction method was used, except that the range was

Table 1 Mean (SD) and range [min max] of the percent of trials rejected per criteria

	% mean (SD)	% range
No Response	2.0 (2.1)	[0 8.8]
Response Error	0.5 (0.5)	[0. 2.0]
Fast RT (< 150ms)	0.3 (0.4)	[0 1.5]
Pedal Down	0.5 (0.8)	[0 3.3]
Force outside ± 0.3N	0.5 (0.7)	[0 3.0]
Force outside 4*SD	4.0 (1.1)	[2 6.2]
Total behavioral (all blocks, n=25)	3.5 (2.8)	[0 12.2]
Total behavioral (blocks rejected, n =5)	18.4 (8.9)	[11 32.2]
Total force	4.6 (1.6)	[2 7.5]

"Pedal down" criterion represents trials where the pedal was depressed prior to stimulus presentation. Shaded areas denote the average percent of trials rejected by behavioral and force criteria. Totals were also calculated for those who did and did not have blocks rejected due to the proportion of successful stops falling below .25 or exceeding .75

now −400 to −200 ms pre-arrow, to avoid edge artifacts produced from the subtraction (Extended Data Fig. 9).

Beta-burst analysis

Raw force data were bandpass-filtered (0.3–30) prior to being convolved with a complex Morlet wavelet (7 cycles), for 15 linearly spaced frequencies (15–29 Hz) in the beta range. Note that this decomposition differs slightly from the one above to match established methods in the beta-burst literature (Wessel, 2020). The squared magnitude of the complex wavelet-convolved data was used to estimate the power. The estimates were then epoched relative to the arrow and response (same time spans as in the force data). Trials marked as behavioral rejections and outliers identified during the force data analysis were removed. Individual peaks in beta power were detected during single trials, using the *imregionalmax* MATLAB function. A peak in beta power was counted as a burst if its amplitude exceeded 3× the median power for that frequency across all trials, based on methods used in Bräcklein et al. (2022).

Electromyography (EMG) analysis

The same trials which were rejected from the force data were also removed from the EMG data. EMG data were then resampled down to 1000 Hz, and the root-mean square was taken at each sample point of every trial. Each trial was then divided by the mean value of its pre-stimulus period (−250 to 0 ms before go signal), before all trials were *z*-scored across all conditions (Raud et al., 2020). This was done separately for left- and right-leg EMG.

Single-trial EMG and force correlations

The single-trial force and EMG data (responding leg only) were averaged into 50 ms segments, from −500 to 500 ms post-arrow. Data were then entered into a mixed model for each 50 ms segment using R (version 4.0.4, packages: car, lme4). The model included force as the dependent variable, and EMG as the independent variable, with subject as the only random effect [$force \sim 1 + emg + (1|subject)$]. This was repeated for each combination of conditions (trial type and arrow direction: Go-L, Go-R, SS-L, SS-R, FS-L, FS-R). For example, the "Go-R" model predicted the subjects' force values (right hand) using their EMG when the go/stop signal pointed right (Fig. 5C).

Coefficient of the variation of force (CVF)

Unfiltered force data were epoched relative to the arrow onset (−500 to 2500 ms). Behavioral rejections and trials rejected during the force analysis were removed. CVF was calculated for each trial, across all time points ($\sigma/\mu * 100$), producing a single CVF value per trial. CVF values were then averaged across trials, to yield a single CVF value per subject, as a measure of individual force unsteadiness. These values were then correlated with subjects' SSRT (Pearson's). A single subject was rejected as an outlier based on Cook's distance (Cook, 1977), leading to the final correlation containing 29 subjects (Fig. 11A, B).

Results

Behavioral results

The reaction time (RT) results are displayed in Fig. 2. Subjects' mean Go RT (580 ms), failed-stop RT (513 ms), and SSRT (309 ms) all showed significant differences from each other when compared using paired-samples *t*-tests (Go vs. FS: $t(29) = 19.9$, $p < .001$; Go vs. SS: $t(29) = 16.7$, $p < .001$; FS vs. SS: $t(29) = 13.3$, $p < .001$).

Isometric force

Significant differences in force output were observed between the three conditions of interest in the following time ranges, corrected for multiple comparisons using the false

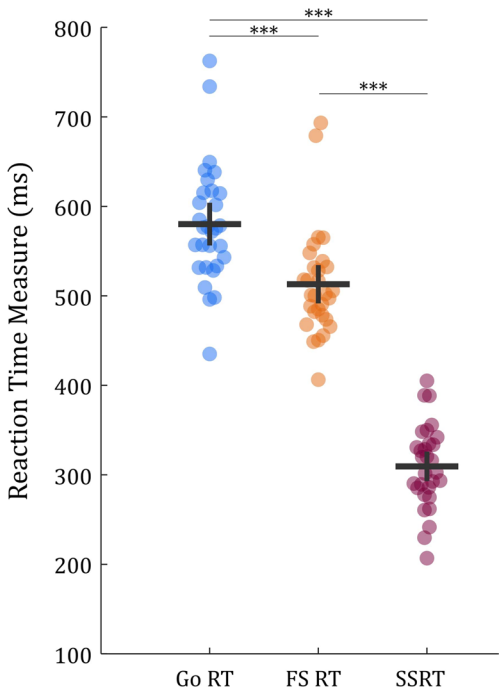

Fig. 2 Average reaction time measures. *Note.* Colored dots denote single subjects' RT measures. Horizontal and vertical lines represent mean and SEM, respectfully. All three conditions differed from each other significantly (***$p < .001$)

discovery rate (FDR) method (Fig. 3A): *Go vs. successful Stop (31–64 ms, 183–390 ms, 411–643 ms, 1350–2500 ms), Go vs. failed Stop (1–2500 ms) and failed vs. successful Stop (1–2079 ms)*. Qualitatively, the force trace for successful stop trials (SS) showed a triphasic pattern highly similar to previous findings where unexpected stimuli were presented to participants during isometric force exertion (Novembre et al., 2018). Here, the pattern was slightly time-delayed, likely due to the visual nature of the stop signal (compared to the lower-latency auditory and haptic stimuli used in Novembre et al., 2018). Notably, the initial dip of this pattern (~150–250 ms post-arrow)—which was larger (more negative) for successful Stop trials than both Go and failed Stop trials (FS) and was largely absent in the force traces of Go and failed Stop trials—preceded the mean SSRT (309 ms post-arrow) of all subjects.

Pearson correlations between the force differences of the conditions (Go-SS, FS-SS, FS-Go) and subjects' SSRT were calculated at every timepoint, with FDR-corrected significant periods highlighted in Fig. 3A (colored bars; time-ranges: Go-SS [36–41 ms, 167–266 ms] and FS-SS [55–503 ms]). To generate a scatter plot, the average differences between conditions were calculated from 183 ms post-arrow (where the initial dip on successful Stop trials began to diverge significantly from the Go condition) to 309 ms post-arrow (the mean SSRT in this sample) and then correlated with SSRT (Fig. 3B). SSRT was highly correlated with differences in force output between Go/SS trials ($r = -.61$, $p < .001$) and FS/SS trials ($r = -.48$, $p = .006$), during this time period.

The unexpected morphology of the FS trial trace—especially its early divergence from the successful Stop and Go trials—suggests that pre-signal differences may distinguish those trials from the other two conditions. Extended Data Fig. 4 (Go-trial locked force traces for all three conditions) shows that this is not the case, as Go and FS trials looked

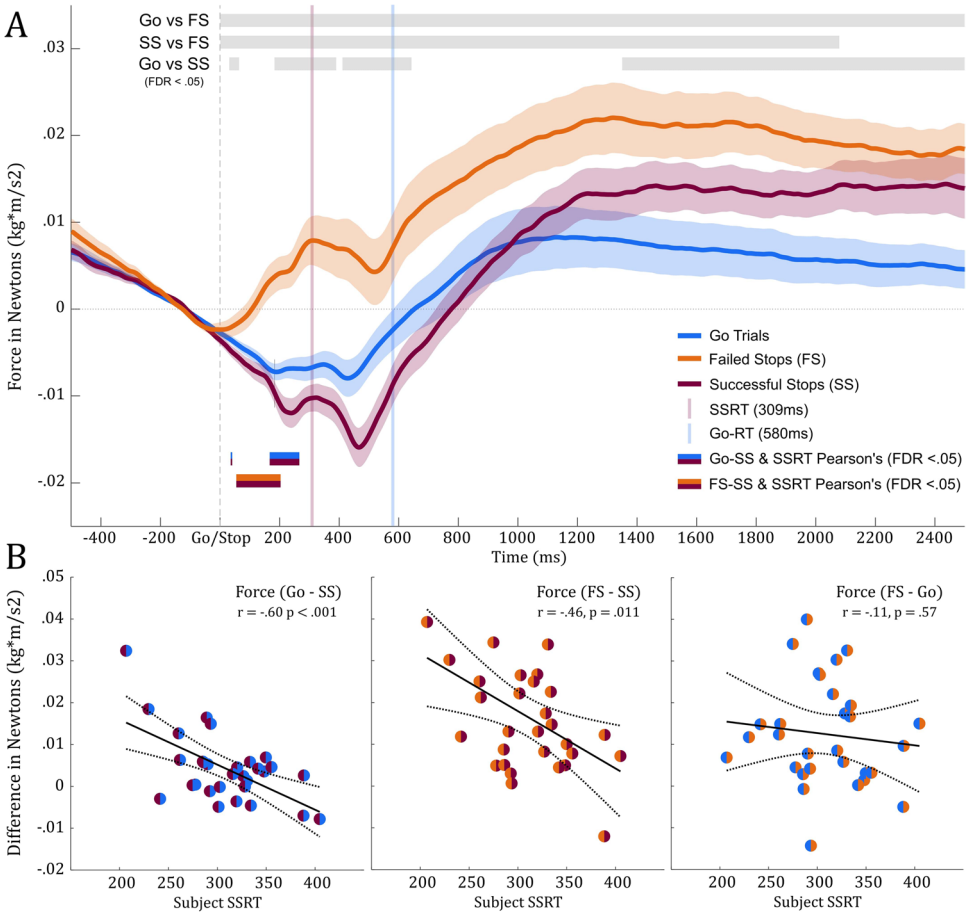

Fig. 3 Average force traces and their relation to SSRT. *Note*. **A** Plot shows the grand mean of force traces for all three conditions (Go, FS, SS), time-locked to the presentation of the relevant stimulus (go signal for Go trials and stop signal for SS and FS trials). Significant differences (FDR < .05) between traces are denoted by gray bars at the top of the plot. Double-colored bars at the bottom of the plot indicate when individual differences in force between conditions significantly correlate with single-subject SSRT. The thin vertical line intersecting the Go and SS force traces marks 183 ms post-arrow, where these conditions begin to differ significantly. **B** Pearson's correlations of the differences between conditions, from 183 ms post-arrow to mean SSRT (309 ms post-arrow) for each subject, and subjects' SSRT

highly similar. Moreover, while the Stop-locked activity was of primary a priori interest in this study, the Go-locked data showed the same force reduction in the successful Stop condition (with additional smearing due to the varying SSD blurring the triphasic pattern observed in the Stop-signal locked data, making the effect look smoother, cf. Extended Data Fig. 4).

Force and EMG: Control analysis

We can see that the EMG data (sampled from the soleus muscle of the responding foot) follow a similar pattern to the force data (sampled from the right hand). Specifically, FS trials exhibit the highest amplitude, while SS trials exhibit the lowest (Fig. 5B). Additionally, individual differences in the EMG conditions did correlate with subjects' SSRT when averaged across the same time period, as was done with the force traces (183–309 ms post-arrow; Extended Data Fig. 6). To address the possibility that the force decreases observed in successful stop trials were caused by passive movement conduction from the foot, we performed a single-trial analysis correlating force and EMG amplitudes. This analysis revealed that subjects' force output and EMG amplitude were positively correlated for right foot responses (Fig. 5C). If the reduction in SS trial force was due to movement conduction from the foot, we would expect this relationship to be negative: more movement (higher EMG) = stronger reduction (lower force). Moreover, for left foot responses, the force-EMG relationship was nonexistent for SS trials, and transiently negative for Go and FS trials, suggesting that this correlation is strongly dependent on which hemisphere is responding. However, when it comes to the force amplitude in SS trials alone (not force-EMG relationship), left and right arrow trials do not exhibit any significant differences from −500 to 1000 ms post-arrow (FDR < .05, Fig. 5D). Thus, while there does exist a significant relationship between force and EMG amplitudes that is dependent on lateralization (see "remote effect"; Kato et al., 2015; Kawakita et al., 1991; Komeilipoor et al., 2017; Tazoe et al., 2009), this relationship does not appear to stem from foot movement artifacts, nor does it alter the drop in force observed in SS trials Fig. 7.

Time-frequency analysis of force trace

Following time-frequency decomposition of the force time series, we observed stimulus-induced modulations of spectral power in both low (~4Hz – Go trials) and high (13–30 Hz – all trials) frequencies, consistent with the results reported by Novembre et al. (2019). Notably, distinct patterns of spectral power can be observed between Go and SS trials. SS trials showed the greatest increase in beta-band power following stimulus presentation, but prior to the mean SSRT (Fig. 8A). Contrasts between conditions showed that the significant differences between Go and SS trials, prior to SSRT, fall almost entirely within the beta-band range (mean $f(\text{Hz}) = 16.1 \pm 4.5$; Fig. 8B). Power differences between conditions were averaged from 183 to 309 ms post-arrow (same as in Fig. 3B) and across frequencies within the beta-band range (13–30 Hz) to produce a single value per contrast and per subject. These

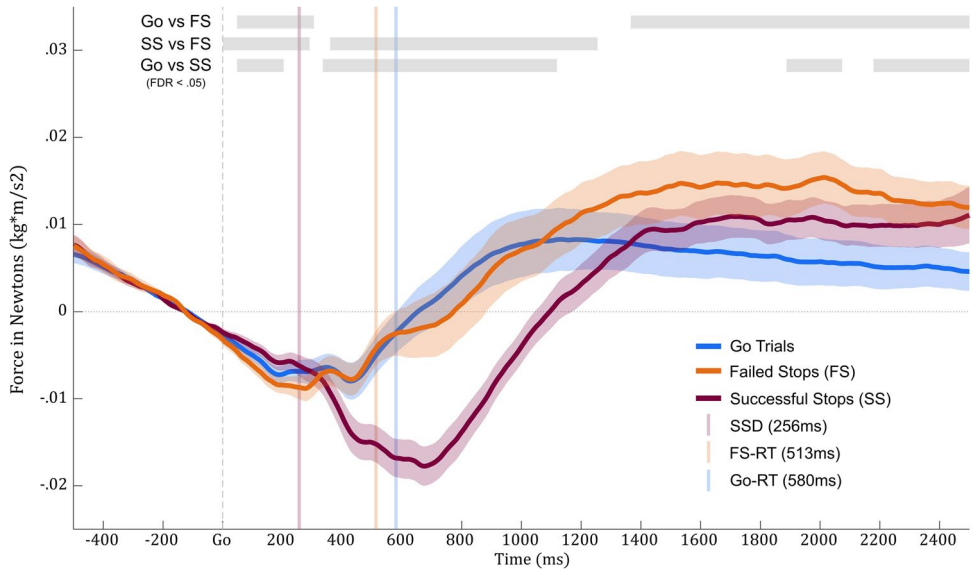

Fig. 4 Average force traces time-locked to the Go stimulus. *Note*. Plot shows the grand mean of force traces for all three conditions (Go, FS, SS), time-locked to the presentation of the go signal for all conditions. Significant differences (FDR < .05) between traces are denoted by gray bars at the top of the plot. Vertical colored lines signify the average stop-signal delay (SSD; 256 ms), failed-stop RT (FS-RT; 513 ms), and Go-RT (580 ms) for all subjects, relative to the presentation of the go signal

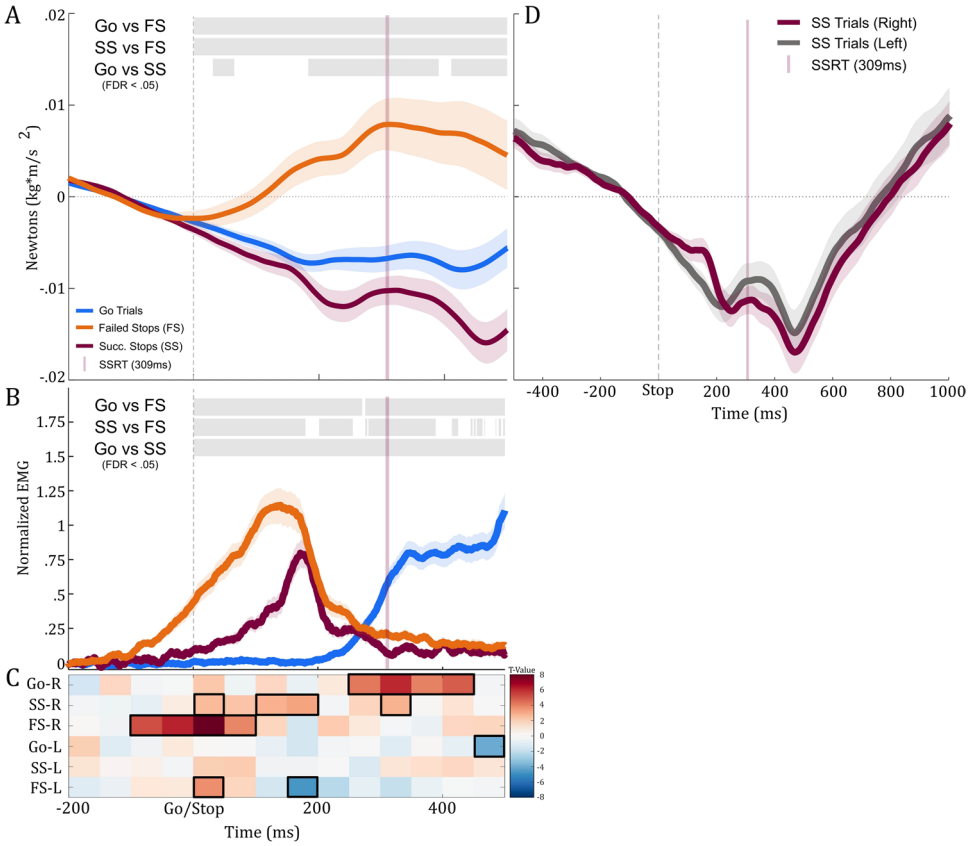

Fig. 5 Average EMG traces and their relation to force output. Note. **A**, **B** Plots show the grand mean of force (right hand) and EMG (responding foot) traces for all three conditions (Go, FS, SS), time-locked to the presentation of the relevant stimulus (go signal for Go trials and stop signal for SS and FS trials). Significant differences (FDR < .05) between traces are denoted by gray bars at the top of the plots. **C** Plot shows the T-values from the single-trial mixed-model analysis, relating the force and EMG amplitudes, for each condition combination. Significant time segments (50 ms; FDR < .05) are outlined in black. **D** Plot shows SS trial force traces for left- and right-facing arrows. Force traces did not differ significantly at any time point (FDR < .05)

values were then correlated with subjects' SSRT (Pearson's; Fig. 8B). Greater differences in power between SS and Go trials predicted faster SSRTs ($r = .46$, $p = .011$).

Furthermore, in a control analysis, we subtracted the average force trace per condition (Go, SS, FS) from the force traces of each trial, prior to time-frequency

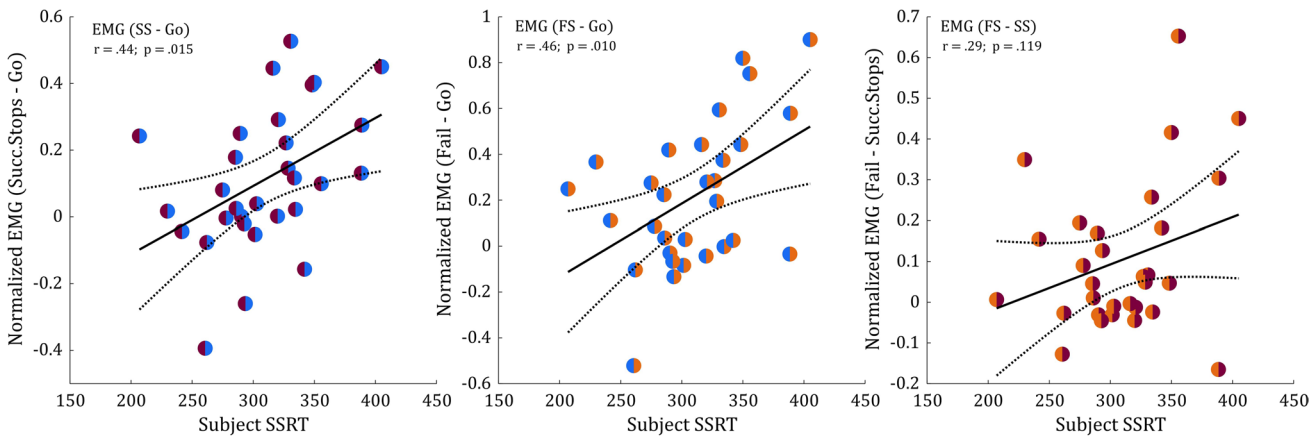

Fig. 6 EMG differences and SSRT. *Note*. Pearson's correlations of the differences in normalized EMG between conditions, from 183 ms post-arrow to mean SSRT (309 ms post-arrow) for each subject, and subjects' SSRT

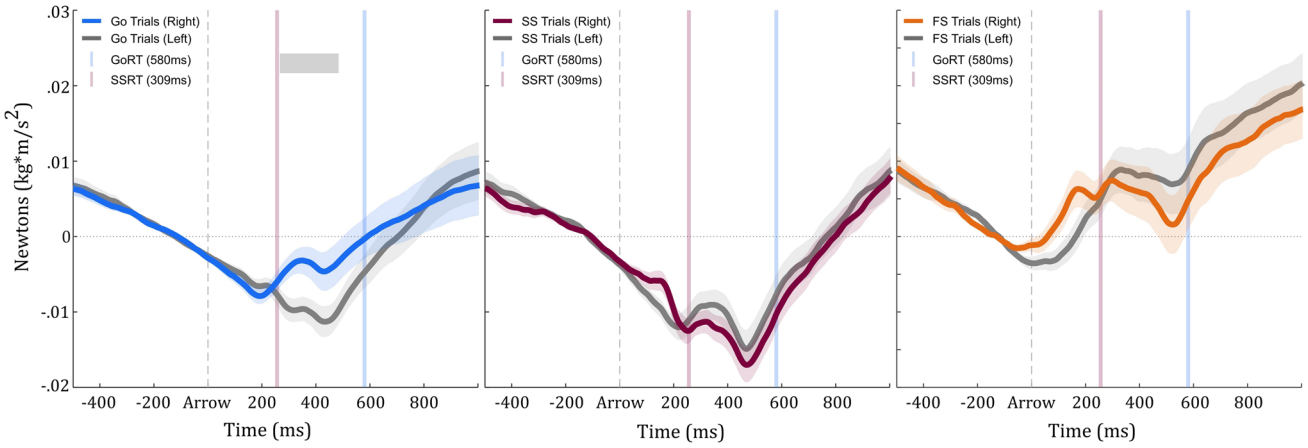

Fig. 7 Force differences based on response lateralization. *Note*. Plots show the force traces for left- and right-facing arrow trials, for all conditions. Only Go trials differed significantly between left and right responses (266–484 ms, FDR < .05)

decomposition. The differences in beta-band power between Go and SS trials remained significant (FDR < .01), as did their relationship with SSRT (Extended Data Fig. 9).

β-Burst rate analysis of isometric force trace

β-burst rate differences were observed during the time span of interest (0–600 ms post-arrow, Fig. 11B). A consistent increase in β-burst rate can be observed in SS trials, compared to Go trials, from 150–250 ms, which temporally coincides with the significant relationship between their force difference (Go-SS) and subject SSRT (Fig. 3A). SS trials show a greater β-burst rate than FS trials, during a narrower time span (150–200 ms post-arrow), before the burst rate for FS trials approaches that of the SS trials in the 200–225 ms time bin Fig. 10.

Coefficient of variation of force (CVF)

The mean coefficient of variation of force was computed across all time points (−500 pre-arrow to 2500 ms post-arrow) and across all trials, for each subject. Following the rejection of one subject (Cook's = .71, Fig. 11B), the remaining 29 subjects' CVF and SSRTs were compared using Pearson's correlation. Greater motor steadiness (lower CVF) significantly predicted faster SSRTs (Fig. 11A).

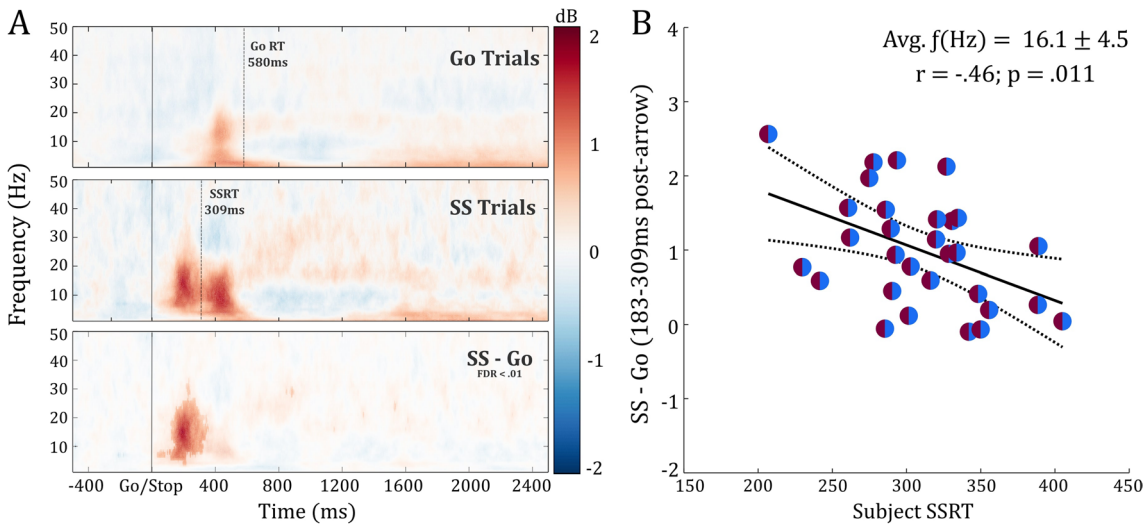

Fig. 8 Results from the time-frequency analysis. *Note*. **A** Plots show the spectral power of the force trace, averaged for Go and SS conditions across subjects, for frequencies 1–50 Hz. Areas of significant difference between Go and SS conditions (FDR < .01) are highlighted in the third panel. **B** The differences between conditions were averaged from 183 to 309 ms post-arrow and across all frequencies within the β-band (13–30 Hz), and compared to single-subject SSRT, using Pearson's correlations. The average frequency (mean ± SD) where Go and SS trials differed significantly are included in the scatter plot

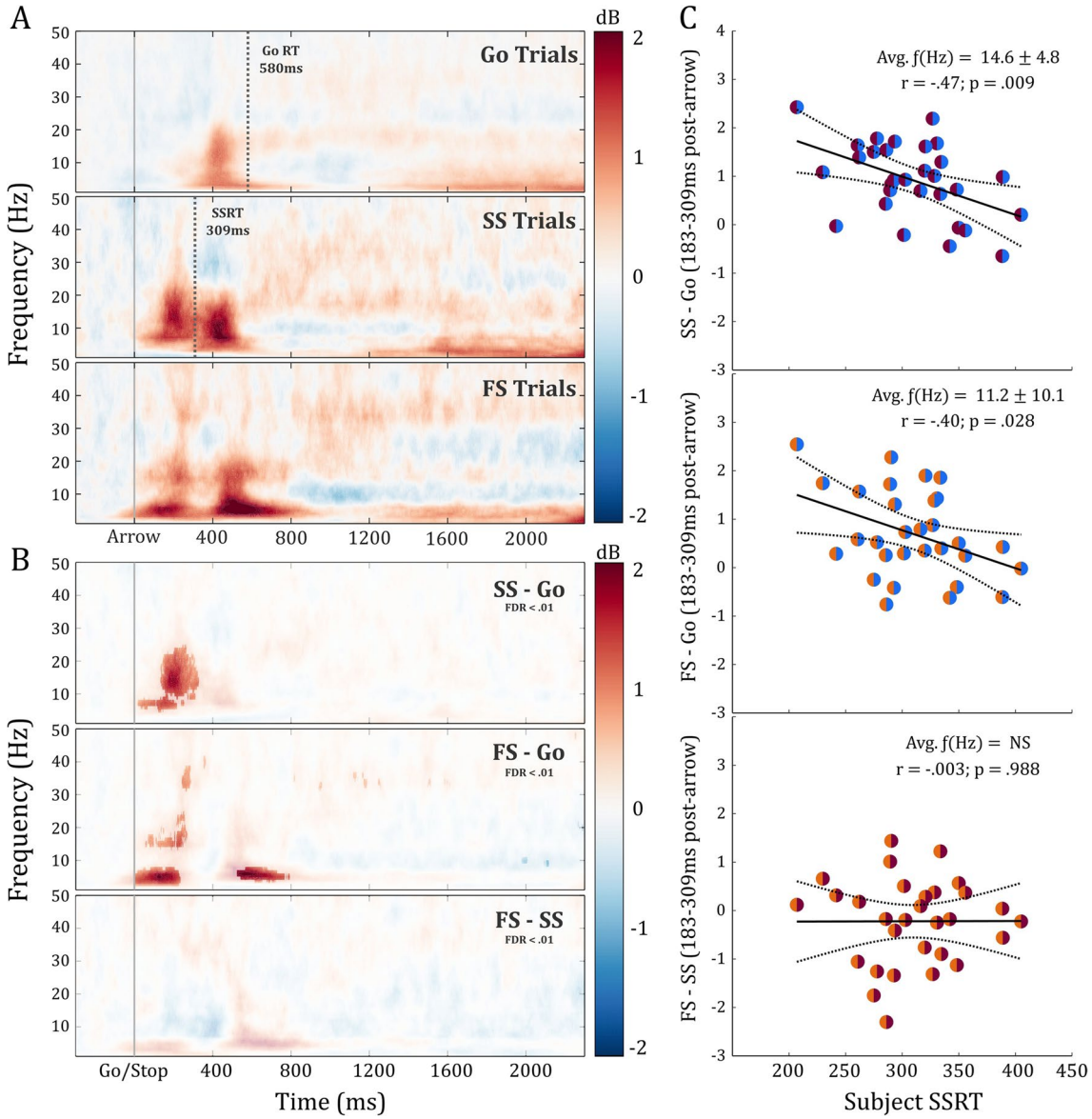

Fig. 9 Time-frequency comparisons for Go, SS, and FS trials. *Note*. **A** Plots show the spectral power of the force trace, averaged for Go, SS, and FS conditions across subjects, after the mean force trace for each condition was subtracted. **B** Areas of significant difference between conditions (FDR < .01) are highlighted. **C** The differences between conditions were averaged from 183 to 309 ms post-arrow and across all frequencies within the β-band (13–30 Hz), and compared to single-subject SSRT, using Pearson's correlations. The average frequencies (mean ± SD) where conditions differed significantly are included in the scatter plots

Considering that SSRT is correlated with both CVF and the differences in force between Go and SS trials (Fig. 3B), we wanted to rule out the possibility that the SSRT-CVF correlation was due to subjects having their differences in force obscured due to their high CVF (force instability). To control for this, we computed the CVF for each subject during the 183–309 post-arrow period and for the whole trial, excluding this period, and compared these values to both SSRT and the differences in force of Go and SS trials (183–309 ms post-arrow) using Pearson's correlations. Two data points were removed from these analyses, based on Cooks' distance, leaving a sample of 28 for the correlations. Subjects' CVF did not correlate significantly with SSRT ($r = .17$, $p = .38$) or differences in force ($r = -.31$, $p = .11$), during the 183–309 ms time span (Fig. 11C). In contrast, the CVF measured outside of this time span (whole-trial, excluding 183–309 ms) did correlate with greater SSRT ($r = .51$, $p = .006$), similar to Fig. 11a, and correlated negatively with Go-SS force differences ($r = -.53$, $p = .003$; Fig. 11C). This further

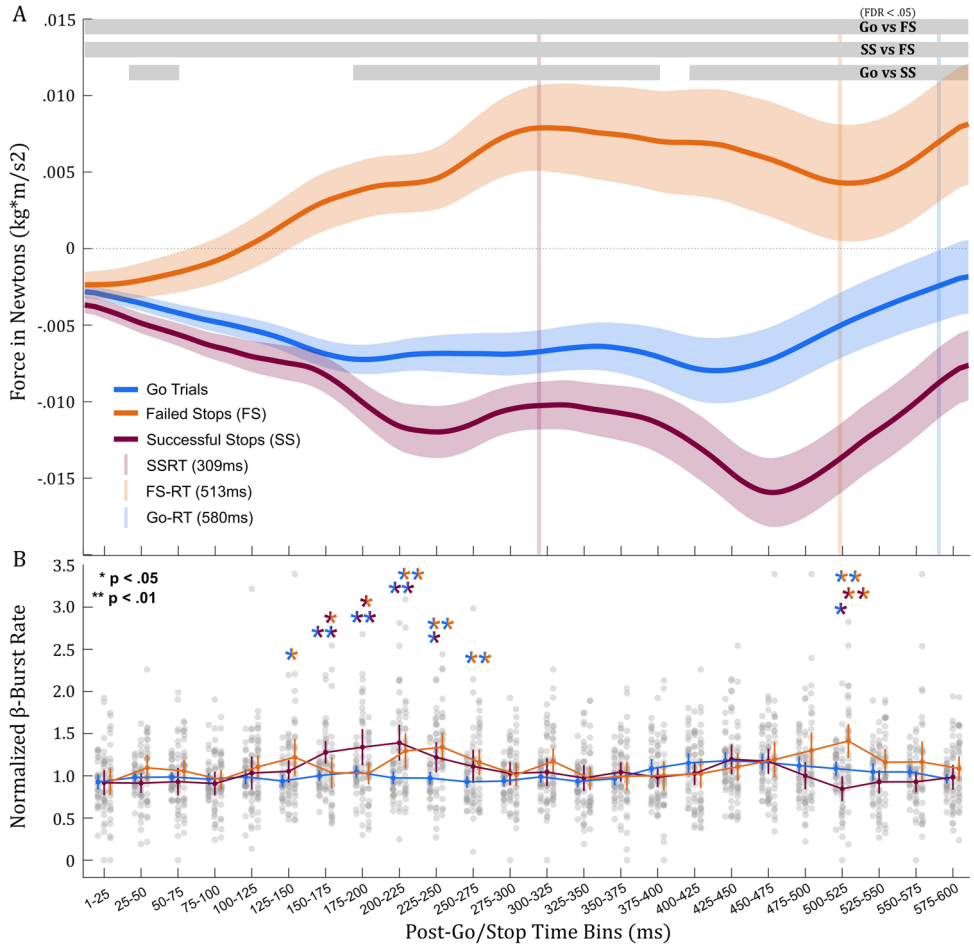

Fig. 10 Force traces and β-burst rate. *Note.* **A** Plot is a zoomed-in version of Fig. 3A–i.e., the time-domain representation of the force trace, limited to the timepoints 0–600 ms post-arrow. Gray bars at the top of the plot indicate significant differences between conditions in the time domain (FDR < .05). **B** Normalized β-burst rates of force data, averaged for each condition, across subjects. Semi-transparent gray dots denote individual subjects' data points. Colored dots represent the mean within each time bin, and are intersected by vertical lines indicating the SEM

supports the idea that subjects with larger CVF values are simply worse at stopping (indexed by both SSRT and phasic force modulation), and not that their differences in force conditions are obscured by force instability.

Finally, we calculated Pearson's partial correlation for subjects' force differences during our window of interest (183–309 ms post-arrow) versus SSRT while controlling for CVF both inside and outside this window (Table 2). While correlations between force differences (Go-SS and FS-SS) were slightly reduced compared to the original correlations (Fig. 3B), they remained significant.

Discussion

In the current study, we tested whether measurements of isometric force could be used to capture the nonselective effects of inhibitory control on the motor system. Indeed, in line with our prediction, data from a foot-response stop-signal task showed that successful stop trials yielded a significant force suppression at the task-unrelated hand prior to stop-signal reaction time, paralleling existing reports of nonselective CSE suppression during action-stopping. Moreover, the magnitude of this suppression was highly predictive of SSRT itself, with subjects who showed faster SSRT also showing stronger short-latency suppression of isometric force. Finally, the force data contained highly useful additional information. First, time-frequency decompositions of the force trace showed a preponderance of beta-band activity during stopping, in line with converging evidence for the importance of this frequency band in motor processes coming from other imaging domains (see below). Second, the coefficient of variation across the entire dataset was also correlated with SSRT. This has important clinical implications, as the CVF has been shown to be elevated in the elderly (Enoka et al., 2003;

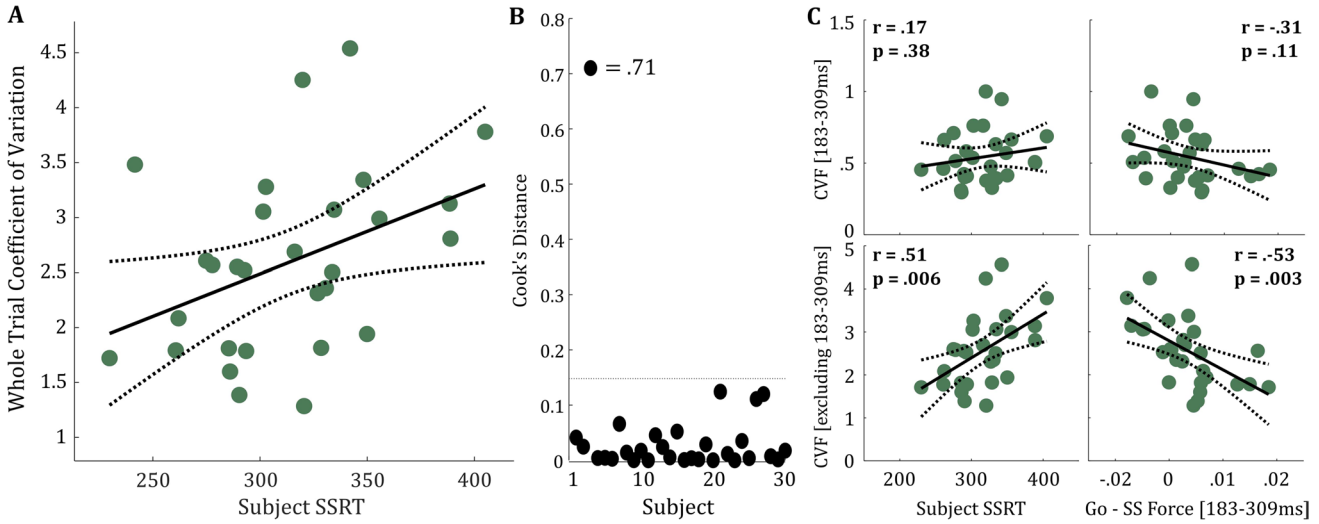

Fig. 11 Coefficient of variation of force and SSRT. *Note.* The relationship between the mean coefficient of variation of force of each subject and their SSRTs. **A** The mean whole-trial (−500 to 2500 ms post-arrow) CVF for each subject was correlated with their SSRTs (Pearson's, $r = .40$, $p = .032$), after the rejection of one outlier (**B**) based on Cook's Distance. **C** Control analyses revealed that only CVF calculated outside of the 183–309 ms post-arrow time span correlated significantly with single subjects' SSRT, and the difference between their Go and SS force traces, during this time span

Galganski et al., 1993) and in Parkinson's disease (Skinner et al., 2019), as well as predictive of poorer coordination (Almuklass et al., 2016) and balance in several clinical populations (Davis et al., 2020; Hyngstrom et al., 2014).

Our main findings mirror those of previous work demonstrating CSE suppression during the stop-signal task. Previous research using TMS has shown that CSE is non-selectively suppressed when participants are able to successfully stop their responses (Badry et al., 2009; Tatz et al., 2021; Wessel et al., 2013; Wessel & Aron, 2017). This suppression is observed approximately 150 ms after the presentation of the stop signal (Jana et al., 2020; Majid et al., 2012; Wessel & Aron, 2017). We observed a commensurate decrease in force output during successful stop trials in the current study. Indeed, this nonselective suppression of isometric force emerged almost exactly 150 ms post-arrow, becoming statistically significant at 183 ms (Fig. 3A). This suppression was relatively small (~0.004 N, or less than 0.5 g), similar to the previous work showing that postural perturbations produce small and short-lasting decreases in motor activity of the hand (Goode et al., 2019). While the suppression of isometric force we observed is likely too modest to interfere with postural control or ongoing static motor output (clutching an item), the individual differences in force output between conditions during this initial suppression period were negatively correlated with single-subject SSRT, beginning at 167 ms. Additionally, these force decreases did not differ based on which foot response was stopped (Fig. 5D), consistent with previous work on the non-selectivity of CSE suppression during action-stopping (Badry et al., 2009; Tatz et al., 2021; Wessel & Aron, 2017). Thus, isometric force recordings provide a temporally precise and highly accurate method for the assessment of nonselective motor suppression during inhibitory control. This is important because force recordings are not affected by many of the common shortcomings associated with TMS-based measurements of CSE. First, unlike TMS methods, force recordings are continuous and allow a quantification of nonselective suppressive effects with dense temporal coverage. This is particularly important since there are meaningful differences in the latency with which the underlying inhibitory control system operates (Chen et al., 2020; Coxon et al., 2012). TMS only allows the collection of a single sample of CSE at one specific time point per trial. Hence, different subjects may show maximal suppression of CSE at slightly different time points. Force recordings can detect such variations by continuously sampling throughout the trial. Second, unlike TMS-based

Table 2 Partial Pearson's correlations between force and SSRT, controlling for CVF

Pearson's Partial Correlation	Controlled for CVF Post-Arrow [183-309ms]		Controlled for CVF Post-Arrow [183-309ms] Excluded	
	r	*p*	*r*	*p*
Go-SS x SSRT	-.54	.003	-.42	.027
Go-FSx SSRT	-.21	.280	-.29	.128
FS-SS x SSRT	-.44	.018	-.45	.017

Partial correlations utilized the standardized residuals

methods, force recordings do not introduce auditory and haptic stimulation to the subject, and are hence potentially less distracting. Third, force recordings do not introduce stimulation artifacts into concurrent neural recordings, and hence do not interfere with other simultaneously acquired data. Fourth, force recordings can be readily performed in populations in which TMS is contraindicated, for example, those with epilepsy, a family history of seizure disorders, or implanted medical devices. Crucially, this can also enable investigations of nonselective motor inhibition using imaging techniques that typically depend on such populations (such as electrocorticography (ECoG), which is only done in epilepsy patients). Fifth, force recordings are comparatively cheap and can be done with minimal footprint. As such, they present a highly viable alternative to TMS-based investigations of the nonselective effects of motor inhibition. Of course, TMS-based methods have other advantages—primarily the fact that the underlying neuronal dynamics of CSE (and other TMS-based indices like intracortical inhibition) are relatively well understood. Future usage of force or TMS-based methods for the quantification of nonselective inhibition will depend on the exact research question, and future research should investigate their potential relevance.

Another advantage of recording densely sampled time-series data from a force transducer is the ability to explore the dynamics of these data in the frequency domain (Novembre et al., 2019). Cortical oscillations in the β-band (13–30 Hz) have long been associated with motor function. A prominent desynchronization of β-band power is observed during movement initiation (McFarland et al., 2000; Pfurtscheller et al., 2003), while increases in β-band power are observed during the cancellation of movements (Picazio et al., 2014; Soh et al., 2021; N. C. Swann et al., 2012; Wagner et al., 2018; Wessel, 2020). Work utilizing both isometric muscular contractions and EEG recordings has revealed a coupling of cortical and motor β-band activity, primarily relegated to the electrode sites contralateral to the active muscle (Bourguignon et al., 2017; Conway et al., 1995; Mongold et al., 2022; Novembre et al., 2019). While some have suggested that this cortico-muscular coherence (CMC) of β-band activity may help maintain consistent motor output directly (Androulidakis et al., 2007; Baker, 2007), and others have proposed that it plays a role in monitoring the periphery via proprioceptive afferent signaling (Bourguignon et al., 2015; Witham et al., 2011), the functional significance of CMC during voluntary contractions is still unclear (Echeverria-Altuna et al., 2022; Ede et al., 2015; Zicher et al., 2022). Here, we found significant differences between conditions by decomposing isometric force data into the time-frequency domain. Most notably, we found that successful Stop trials showed increased β-band activity compared to Go trials, and that these differences predicted single-subject SSRT (Fig. 10). Recently, the measurement of cortical β-band activity has shifted towards single-trial estimation of burst-like events, rather than trial-averaged changes in power. Previous research has shown that β-activity is characterized as transient bursts, rather than prolonged changes (Bonaiuto et al., 2021; Feingold et al., 2015; Leventhal et al., 2012; Sherman et al., 2016), and the presence or absence of these β-bursts better predicts behavior (Shin et al., 2017; Soh et al., 2021; Wessel, 2020). We compared the rate of β-bursts for each condition and showed that the bursting rate for successful Stop trials was significantly greater than those of failed Stop and Go trials, from 150 to 200 ms post-arrow (Fig. 10). A delayed increase in β-burst rate for failed Stop trials followed by about 50 ms. This finding is consistent with the idea that burst rates indicate more successful movement cancelation, as well as studies suggesting that β-bursts propagate to contracting muscles (Bräcklein et al., 2022; Echeverria-Altuna et al., 2022).

Finally, our exploratory analysis of the coefficient of variation of force (CVF) highlights additional potential applications of isometric force measurements. The CVF of isometric force data has long been associated with a variety of clinical measures (Enoka & Farina, 2021). Greater CVF has been shown to accompany poorer performance on walking tests (Mani et al., 2018), grooved pegboard tests (Almuklass et al., 2016; Feeney et al., 2018), and assessments of postural sway (Kouzaki & Shinohara, 2010), especially in elderly patients. Increased CVF has also been associated with greater symptomology in Parkinson's disease (Wilson et al., 2020), stroke survivors (Hyngstrom et al., 2014), and patients with multiple sclerosis (Davis et al., 2020). While some studies have explored the modulation of CVF due to task conditions or stimuli presentation (Christou et al., 2004; Farina et al., 2012), it remains relatively unexplored in relation to higher cognition and nonclinical assessments. Here, we demonstrated that the averaged whole-trial CVF for each subject was positively correlated with SSRT. Hence, performance metrics in the stop-signal task may provide a potential complementary window into these clinical assessments.

In sum, we report herein a novel signature of the nonselective effects of inhibitory control on the motor system. Isometric force recordings from a task-unrelated motor effector showed a clear reduction in force when another effector was successfully stopped. Moreover, the degree of this suppression was strongly correlated with participants' stopping ability. Unlike the previous gold-standard method used to demonstrate such nonselective motor effects (TMS-based CSE recordings), isometric force recordings provide high temporal resolution, superior compatibility with other imaging methods, applicability in previously inaccessible populations, minimal distraction to the subject, a small footprint, and low cost. Future work should capitalize on these properties to study the neural underpinnings of the nonselective effects of inhibitory control on the motor system.

Acknowledgements This work was funded by the National Science Foundation (NSF CAREER 1752355 to JRW). GN acknowledges support from the European Research Council (grant agreement 948186).

The data and materials reported here are available on the Open Science Framework (https://osf.io/en8t9/) This experiment was not preregistered.

Funding National Science Foundation (NSF CAREER 1752355 to JRW).

Data availability https://osf.io/en8t9/.

Code availability https://osf.io/en8t9/.

Declarations

Conflict of interest The authors report no financial conflict of interest.

Ethics approval University of Iowa (IRB #201511709).

Consent to participate Informed consent was obtained from all individual participants in the study.

Consent for publication Participants gave informed consent as to the publishing of their data.

References

Almuklass, A. M., Price, R. C., Gould, J. R., & Enoka, R. M. (2016). Force steadiness as a predictor of time to complete a pegboard test of dexterity in young men and women. *Journal of Applied Physiology, 120*(12), 1410–1417. https://doi.org/10.1152/japplphysiol.01051.2015

Androulidakis, A. G., Doyle, L. M. F., Yarrow, K., Litvak, V., Gilbertson, T. P., & Brown, P. (2007). Anticipatory changes in beta synchrony in the human corticospinal system and associated improvements in task performance. *European Journal of Neuroscience, 25*(12), 3758–3765. https://doi.org/10.1111/j.1460-9568.2007.05620.x

Aron, A. R., & Poldrack, R. A. (2006). Cortical and subcortical contributions to stop signal response inhibition: Role of the subthalamic nucleus. *The Journal of Neuroscience, 26*(9), 2424–2433. https://doi.org/10.1523/jneurosci.4682-05.2006

Badawy, R. A. B., Jackson, G. D., Berkovic, S. F., & MacDonell, R. A. L. (2013). Cortical excitability and refractory epilepsy: A three-year longitudinal transcranial magnetic stimulation study. *International Journal of Neural Systems, 23*(01), 1250030. https://doi.org/10.1142/s012906571250030x

Badry, R., Mima, T., Aso, T., Nakatsuka, M., Abe, M., Fathi, D., Foly, N., Nagiub, H., Nagamine, T., & Fukuyama, H. (2009). Suppression of human cortico-motoneuronal excitability during the stop-signal task. *Clinical Neurophysiology, 120*(9), 1717–1723. https://doi.org/10.1016/j.clinph.2009.06.027

Baker, S. N. (2007). Oscillatory interactions between sensorimotor cortex and the periphery. *Current Opinion in Neurobiology, 17*(6), 649–655. https://doi.org/10.1016/j.conb.2008.01.007

Bestmann, S., & Duque, J. (2016). Transcranial magnetic stimulation: Decomposing the processes underlying action preparation. *The Neuroscientist, 22*(4), 392–405. https://doi.org/10.1177/1073858415592594

Bonaiuto, J. J., Little, S., Neymotin, S. A., Jones, S. R., Barnes, G. R., & Bestmann, S. (2021). Laminar dynamics of high amplitude beta bursts in human motor cortex. *NeuroImage, 242*, 118479. https://doi.org/10.1016/j.neuroimage.2021.118479

Bourguignon, M., Piitulainen, H., Smeds, E., Zhou, G., Jousmäki, V., & Hari, R. (2017). MEG insight into the spectral dynamics underlying steady isometric muscle contraction. *The Journal of Neuroscience, 37*(43), 10421–10437. https://doi.org/10.1523/jneurosci.0447-17.2017

Bourguignon, M., Piitulainen, H., Tiège, X. D., Jousmäki, V., & Hari, R. (2015). Corticokinematic coherence mainly reflects movement-induced proprioceptive feedback. *NeuroImage, 106*, 382–390. https://doi.org/10.1016/j.neuroimage.2014.11.026

Bräcklein, M., Barsakcioglu, D. Y., Vecchio, A. D., Ibáñez, J., & Farina, D. (2022). Reading and modulating cortical β bursts from motor unit spiking activity. *The Journal of Neuroscience, 42*(17), 3611–3621. https://doi.org/10.1523/jneurosci.1885-21.2022

Brainard, D. H. (1997). The psychophysics toolbox. *Spatial Vision, 10*(4), 433–436. https://doi.org/10.1163/156856897x00357

Cavanagh, J. F., Sanguinetti, J. L., Allen, J. J. B., Sherman, S. J., & Frank, M. J. (2014). The subthalamic nucleus contributes to post-error slowing. *Journal of Cognitive Neuroscience, 26*(11), 2637–2644. https://doi.org/10.1162/jocn_a_00659

Chen, W., de Hemptinne, C., Miller, A. M., Leibbrand, M., Little, S. J., Lim, D. A., Larson, P. S., & Starr, P. A. (2020). Prefrontal-subthalamic Hyperdirect pathway modulates movement inhibition in humans. *Neuron, 106*(4), 579–588.e3. https://doi.org/10.1016/j.neuron.2020.02.012

Chowdhury, N. S., Livesey, E. J., Blaszczynski, A., & Harris, J. A. (2018). Variations in response control within at-risk gamblers and non-gambling controls explained by GABAergic inhibition in the motor cortex. *Cortex, 103*, 153–163. https://doi.org/10.1016/j.cortex.2018.03.004

Christou, E. A., Jakobi, J. M., Critchlow, A., Fleshner, M., & Enoka, R. M. (2004). The 1- to 2-Hz oscillations in muscle force are exacerbated by stress, especially in older adults. *Journal of Applied Physiology, 97*(1), 225–235. https://doi.org/10.1152/japplphysiol.00066.2004

Conway, B. A., Halliday, D. M., Farmer, S. F., Shahani, U., Maas, P., Weir, A. I., & Rosenberg, J. R. (1995). Synchronization between motor cortex and spinal motoneuronal pool during the performance of a maintained motor task in man. *The Journal of Physiology, 489*(3), 917–924. https://doi.org/10.1113/jphysiol.1995.sp021104

Cook, R. D. (1977). Detection of influential observation in linear regression. *Technometrics, 19*(1), 15–18. https://doi.org/10.1080/00401706.1977.10489493

Coxon, J. P., Impe, A. V., Wenderoth, N., & Swinnen, S. P. (2012). Aging and inhibitory control of action: Cortico-subthalamic connection strength predicts stopping performance. *Journal of Neuroscience, 32*(24), 8401–8412. https://doi.org/10.1523/jneurosci.6360-11.2012

Coxon, J. P., Stinear, C. M., & Byblow, W. D. (2006). Intracortical inhibition during volitional inhibition of prepared action. *Journal of Neurophysiology, 95*(6), 3371–3383. https://doi.org/10.1152/jn.01334.2005

Davis, L. A., Alenazy, M. S., Almuklass, A. M., Feeney, D. F., Vieira, T., Botter, A., & Enoka, R. M. (2020). Force control during submaximal isometric contractions is associated with walking performance in persons with multiple sclerosis. *Journal of Neurophysiology, 123*(6), 2191–2200. https://doi.org/10.1152/jn.00085.2020

Dutra, I. C., Waller, D. A., & Wessel, J. R. (2018). Perceptual surprise improves action stopping by nonselectively suppressing motor activity via a neural mechanism for motor inhibition. *Journal of Neuroscience, 38*(6), 1482–1492. https://doi.org/10.1523/jneurosci.3091-17.2017

Echeverria-Altuna, I., Quinn, A. J., Zokaei, N., Woolrich, M. W., Nobre, A. C., & Ede, F. van. (2022). Transient beta activity and cortico-muscular connectivity during sustained motor behaviour. *Progress in Neurobiology*, *214*, 102281. https://doi.org/10.1016/j.pneurobio.2022.102281

Ede, F. van, Winner, T., & Maris, E. (2015). Touch automatically upregulates motor readiness in humans. *Journal of Neurophysiology*, *114*(6), 3121–3130. https://doi.org/10.1152/jn.00504.2015

Enoka, R. M., Christou, E. A., Hunter, S. K., Kornatz, K. W., Semmler, J. G., Taylor, A. M., & Tracy, B. L. (2003). Mechanisms that contribute to differences in motor performance between young and old adults. *Journal of Electromyography and Kinesiology, 13*(1), 1–12. https://doi.org/10.1016/s1050-6411(02)00084-6

Enoka, R. M., & Farina, D. (2021). Force steadiness: From motor units to voluntary actions. *Physiology, 36*(2), 114–130. https://doi.org/10.1152/physiol.00027.2020

Erika-Florence, M., Leech, R., & Hampshire, A. (2014). A functional network perspective on response inhibition and attentional control. *Nature Communications, 5*(1), 4073. https://doi.org/10.1038/ncomms5073

Farina, D., Negro, F., Gizzi, L., & Falla, D. (2012). Low-frequency oscillations of the neural drive to the muscle are increased with experimental muscle pain. *Journal of Neurophysiology, 107*(3), 958–965. https://doi.org/10.1152/jn.00304.2011

Feeney, D. F., Mani, D., & Enoka, R. M. (2018). Variability in common synaptic input to motor neurons modulates both force steadiness and pegboard time in young and older adults. *The Journal of Physiology, 596*(16), 3793–3806. https://doi.org/10.1113/jp275658

Feingold, J., Gibson, D. J., DePasquale, B., & Graybiel, A. M. (2015). Bursts of beta oscillation differentiate postperformance activity in the striatum and motor cortex of monkeys performing movement tasks. *Proceedings of the National Academy of Sciences, 112*(44), 13687–13692. https://doi.org/10.1073/pnas.1517629112

Fiori, F., Chiappini, E., Candidi, M., Romei, V., Borgomaneri, S., & Avenanti, A. (2017). Long-latency interhemispheric interactions between motor-related areas and the primary motor cortex: A dual site TMS study. *Scientific Reports, 7*(1), 14936. https://doi.org/10.1038/s41598-017-13708-2

Fitzgerald, P. B., Fountain, S., & Daskalakis, Z. J. (2006). A comprehensive review of the effects of rTMS on motor cortical excitability and inhibition. *Clinical Neurophysiology, 117*(12), 2584–2596. https://doi.org/10.1016/j.clinph.2006.06.712

Frank, M. J., Samanta, J., Moustafa, A. A., & Sherman, S. J. (2007). Hold your horses: Impulsivity, deep brain stimulation, and medication in parkinsonism. *Science, 318*(5854), 1309–1312. https://doi.org/10.1126/science.1146157

Galganski, M. E., Fuglevand, A. J., & Enoka, R. M. (1993). Reduced control of motor output in a human hand muscle of elderly subjects during submaximal contractions. *Journal of Neurophysiology, 69*(6), 2108–2115. https://doi.org/10.1152/jn.1993.69.6.2108

Goode, C., Cole, D. M., & Bolton, D. A. E. (2019). Staying upright by shutting down? Evidence for global suppression of the motor system when recovering balance. *Gait & Posture, 70*, 260–263. https://doi.org/10.1016/j.gaitpost.2019.03.018

Guan, Y., & Wessel, J. R. (2022). Two types of motor inhibition after action errors in humans. *The journal of neuroscience*, JN-RM-1191-22. https://doi.org/10.1523/jneurosci.1191-22.2022.

Hallett, M., & Chokroverty, S. (2006). Magnetic stimulation in clinical neurophysiology. 2nd ed. *American Journal of Neuroradiology*, *27*(8), 1799. http://www.ajnr.org/content/27/8/1799.abstract. Accessed 16 Oct 2022

Hamada, M., Galea, J. M., Lazzaro, V. D., Mazzone, P., Ziemann, U., & Rothwell, J. C. (2014). Two distinct interneuron circuits in human motor cortex are linked to different subsets of physiological and behavioral plasticity. *The Journal of Neuroscience, 34*(38), 12837–12849. https://doi.org/10.1523/jneurosci.1960-14.2014

Hannah, R., & Rothwell, J. C. (2017). Pulse duration as well as current direction determines the specificity of transcranial magnetic stimulation of motor cortex during contraction. *Brain Stimulation, 10*(1), 106–115. https://doi.org/10.1016/j.brs.2016.09.008

Herz, D. M., Tan, H., Brittain, J.-S., Fischer, P., Cheeran, B., Green, A. L., FitzGerald, J., Aziz, T. Z., Ashkan, K., Little, S., Foltynie, T., Limousin, P., Zrinzo, L., Bogacz, R., & Brown, P. (2017). Distinct mechanisms mediate speed-accuracy adjustments in cortico-subthalamic networks. *ELife, 6*, e21481. https://doi.org/10.7554/elife.21481

Hyngstrom, A. S., Kuhnen, H. R., Kirking, K. M., & Hunter, S. K. (2014). Functional implications of impaired control of submaximal hip flexion following stroke. *Muscle & Nerve, 49*(2), 225–232. https://doi.org/10.1002/mus.23886

Ilmoniemi, R. J., Hernandez-Pavon, J. C., Mäkelä, N. N., Metsomaa, J., Mutanen, T. P., Stenroos, M., & Sarvas, J. (2015). Dealing with artifacts in TMS-evoked EEG. In *2015 37th annual international conference of the IEEE engineering in medicine and biology society (EMBC), 2015* (pp. 230–233). https://doi.org/10.1109/embc.2015.7318342

Jahanshahi, M., & Rothwell, J. C. (2017). Inhibitory dysfunction contributes to some of the motor and non-motor symptoms of movement disorders and psychiatric disorders. *Philosophical Transactions of the Royal Society of London. Series B, Biological Sciences, 372*(1718), 20160198. https://doi.org/10.1098/rstb.2016.0198

Jana, S., Hannah, R., Muralidharan, V., & Aron, A. R. (2020). Temporal cascade of frontal, motor and muscle processes underlying human action-stopping. *ELife, 9*, e50371. https://doi.org/10.7554/elife.50371

Jong, R. D., Coles, M. G. H., Logan, G. D., & Gratton, G. (1990). In search of the point of no return: The control of response processes. *Journal of Experimental Psychology: Human Perception and Performance, 16*(1), 164–182. https://doi.org/10.1037/0096-1523.16.1.164

Kato, K., Watanabe, T., & Kanosue, K. (2015). Effects of muscle relaxation on sustained contraction of ipsilateral remote muscle. *Physiological Reports, 3*(11), e12620. https://doi.org/10.14814/phy2.12620

Kawakita, H., Kameyama, O., Ogawa, R., Hayes, K. C., Wolfe, D. L., & Allatt, R. D. (1991). Reinforcement of motor evoked potentials by remote muscle contraction. *Journal of Electromyography and Kinesiology, 1*(2), 96–106. https://doi.org/10.1016/1050-6411(91)90003-n

Kok, A., Ramautar, J. R., Ruiter, M. B. D., Band, G. P. H., & Ridderinkhof, K. R. (2004). ERP components associated with successful and unsuccessful stopping in a stop-signal task. *Psychophysiology, 41*(1), 9–20. https://doi.org/10.1046/j.1469-8986.2003.00127.x

Komeilipoor, N., Ilmoniemi, R. J., Tiippana, K., Vainio, M., Tiainen, M., & Vainio, L. (2017). Preparation and execution of teeth clenching and foot muscle contraction influence on corticospinal hand-muscle excitability. *Scientific Reports, 7*(1), 41249. https://doi.org/10.1038/srep41249

Kouzaki, M., & Shinohara, M. (2010). Steadiness in plantar flexor muscles and its relation to postural sway in young and elderly adults. *Muscle & Nerve, 42*(1), 78–87. https://doi.org/10.1002/mus.21599

Lazzaro, V. D., & Rothwell, J. C. (2014). Corticospinal activity evoked and modulated by non-invasive stimulation of the intact human motor cortex. *The Journal of Physiology, 592*(19), 4115–4128. https://doi.org/10.1113/jphysiol.2014.274316

Leocani, L., Cohen, L. G., Wassermann, E. M., Ikoma, K., & Hallett, M. (2000). Human corticospinal excitability evaluated with transcranial magnetic stimulation during different reaction time

paradigms. *Brain, 123*(6), 1161–1173. https://doi.org/10.1093/brain/123.6.1161

Leventhal, D. K., Gage, G. J., Schmidt, R., Pettibone, J. R., Case, A. C., & Berke, J. D. (2012). Basal ganglia Beta oscillations accompany Cue utilization. *Neuron, 73*(3), 523–536. https://doi.org/10.1016/j.neuron.2011.11.032

Logan, G. D., Cowan, W. B., & Davis, K. A. (1984). On the ability to inhibit simple and choice reaction time responses: A model and a method. *Journal of Experimental Psychology: Human Perception and Performance, 10*(2), 276–291. https://doi.org/10.1037/0096-1523.10.2.276

Majid, D. S. A., Cai, W., George, J. S., Verbruggen, F., & Aron, A. R. (2012). Transcranial magnetic stimulation reveals dissociable mechanisms for global versus selective Corticomotor suppression underlying the stopping of action. *Cerebral Cortex, 22*(2), 363–371. https://doi.org/10.1093/cercor/bhr112

Mani, D., Almuklass, A. M., Hamilton, L. D., Vieira, T. M., Botter, A., & Enoka, R. M. (2018). Motor unit activity, force steadiness, and perceived fatigability are correlated with mobility in older adults. *Journal of Neurophysiology, 120*(4), 1988–1997. https://doi.org/10.1152/jn.00192.2018

Matzke, D., Verbruggen, F., & Logan, G. D. (2018). *Stevens' handbook of experimental psychology and cognitive neuroscience*. 1–45. https://doi.org/10.1002/9781119170174.epcn510.

McFarland, D. J., Miner, L. A., Vaughan, T. M., & Wolpaw, J. R. (2000). Mu and Beta rhythm topographies during motor imagery and actual movements. *Brain Topography, 12*(3), 177–186. https://doi.org/10.1023/a:1023437823106

Miocinovic, S., Hemptinne, C. de, Chen, W., Isbaine, F., Willie, J. T., Ostrem, J. L., & Starr, P. A. (2018). Cortical potentials evoked by subthalamic stimulation demonstrate a short latency Hyperdirect pathway in humans. *The Journal of Neuroscience*, *38*(43), 9129–9141. https://doi.org/10.1523/jneurosci.1327-18.2018

Mongold, S. J., Piitulainen, H., Legrand, T., Ghinst, M. V., Naeije, G., Jousmäki, V., & Bourguignon, M. (2022). Temporally stable beta sensorimotor oscillations and corticomuscular coupling underlie force steadiness. *NeuroImage, 261*, 119491. https://doi.org/10.1016/j.neuroimage.2022.119491

Nambu, A., Tokuno, H., & Takada, M. (2002). Functional significance of the cortico–subthalamo–pallidal 'hyperdirect' pathway. *Neuroscience Research, 43*(2), 111–117. https://doi.org/10.1016/s0168-0102(02)00027-5

Novembre, G., & Iannetti, G. D. (2021). Towards a unified neural mechanism for reactive adaptive behaviour. *Progress in Neurobiology, 204*, 102115. https://doi.org/10.1016/j.pneurobio.2021.102115

Novembre, G., Pawar, V., Bufacchi, R., Kilintari, M., Srinivasan, M., Rothwell, J., Haggard, P., & Iannetti, G. (2018). Saliency detection as a reactive process: Unexpected sensory events evoke corticomuscular coupling. *Journal of Neuroscience, 38*(9), 2474–2417. https://doi.org/10.1523/jneurosci.2474-17.2017

Novembre, G., Pawar, V. M., Kilintari, M., Bufacchi, R. J., Guo, Y., Rothwell, J. C., & Iannetti, G. D. (2019). The effect of salient stimuli on neural oscillations, isometric force, and their coupling. *NeuroImage, 198*, 221–230. https://doi.org/10.1016/j.neuroimage.2019.05.032

Pfurtscheller, G., Graimann, B., Huggins, J. E., Levine, S. P., & Schuh, L. A. (2003). Spatiotemporal patterns of beta desynchronization and gamma synchronization in corticographic data during self-paced movement. *Clinical Neurophysiology, 114*(7), 1226–1236. https://doi.org/10.1016/s1388-2457(03)00067-1

Picazio, S., Veniero, D., Ponzo, V., Caltagirone, C., Gross, J., Thut, G., & Koch, G. (2014). Prefrontal control over Motor cortex cycles at Beta frequency during movement inhibition. *Current Biology, 24*(24), 2940–2945. https://doi.org/10.1016/j.cub.2014.10.043

Raud, L., Huster, R. J., Ivry, R. B., Labruna, L., Messel, M. S., & Greenhouse, I. (2020). A single mechanism for global and selective response inhibition under the influence of motor preparation. *The Journal of Neuroscience, 40*(41), 7921–7935. https://doi.org/10.1523/jneurosci.0607-20.2020

Rogasch, N. C., Sullivan, C., Thomson, R. H., Rose, N. S., Bailey, N. W., Fitzgerald, P. B., Farzan, F., & Hernandez-Pavon, J. C. (2017). Analysing concurrent transcranial magnetic stimulation and electroencephalographic data: A review and introduction to the open-source TESA software. *NeuroImage, 147*, 934–951. https://doi.org/10.1016/j.neuroimage.2016.10.031

Rossi, S., Antal, A., Bestmann, S., Bikson, M., Brewer, C., Brockmöller, J., Carpenter, L. L., Cincotta, M., Chen, R., Daskalakis, J. D., Lazzaro, V. D., Fox, M. D., George, M. S., Gilbert, D., Kimiskidis, V. K., Koch, G., Ilmoniemi, R. J., Lefaucheur, J. P., Leocani, L., et al. (2020). T. basis of this article began with a C. S. from the I. W. on "Present, Future of TMS: Safety, Ethical Guidelines", Siena, October 17-20, 2018, updating through April. (2020). Safety and recommendations for TMS use in healthy subjects and patient populations, with updates on training, ethical and regulatory issues: Expert Guidelines. *Clinical Neurophysiology, 132*(1), 269–306. https://doi.org/10.1016/j.clinph.2020.10.003

Sherman, M. A., Lee, S., Law, R., Haegens, S., Thorn, C. A., Hämäläinen, M. S., Moore, C. I., & Jones, S. R. (2016). Neural mechanisms of transient neocortical beta rhythms: Converging evidence from humans, computational modeling, monkeys, and mice. *Proceedings of the National Academy of Sciences, 113*(33), E4885–E4894. https://doi.org/10.1073/pnas.1604135113

Shin, H., Law, R., Tsutsui, S., Moore, C. I., & Jones, S. R. (2017). The rate of transient beta frequency events predicts behavior across tasks and species. *ELife, 6*, e29086. https://doi.org/10.7554/elife.29086

Siegert, S., Ruiz, M. H., Brücke, C., Huebl, J., Schneider, G.-H., Ullsperger, M., & Kühn, A. A. (2014). Error signals in the subthalamic nucleus are related to post-error slowing in patients with Parkinson's disease. *Cortex, 60*, 103–120. https://doi.org/10.1016/j.cortex.2013.12.008

Skinner, J. W., Christou, E. A., & Hass, C. J. (2019). Lower extremity muscle strength and force variability in persons with Parkinson disease. *Journal of Neurologic Physical Therapy, 43*(1), 56–62. https://doi.org/10.1097/npt.0000000000000244

Smith, M.-C., & Stinear, C. M. (2016). Transcranial magnetic stimulation (TMS) in stroke: Ready for clinical practice? *Journal of Clinical Neuroscience, 31*, 10–14. https://doi.org/10.1016/j.jocn.2016.01.034

Soh, C., Hynd, M., Rangel, B. O., & Wessel, J. R. (2021). Adjustments to proactive motor inhibition without effector-specific foreknowledge are reflected in a bilateral upregulation of sensorimotor β-burst rates. *Journal of Cognitive Neuroscience, 33*(5), 784–798. https://doi.org/10.1162/jocn_a_01682

Swann, N. C., Cai, W., Conner, C. R., Pieters, T. A., Claffey, M. P., George, J. S., Aron, A. R., & Tandon, N. (2012). Roles for the pre-supplementary motor area and the right inferior frontal gyrus in stopping action: Electrophysiological responses and functional and structural connectivity. *NeuroImage, 59*(3), 2860–2870. https://doi.org/10.1016/j.neuroimage.2011.09.049

Swann, N., Tandon, N., Canolty, R., Ellmore, T. M., McEvoy, L. K., Dreyer, S., DiSano, M., & Aron, A. R. (2009). Intracranial EEG reveals a time- and frequency-specific role for the right inferior frontal gyrus and primary motor cortex in stopping initiated responses. *Journal of Neuroscience, 29*(40), 12675–12685. https://doi.org/10.1523/jneurosci.3359-09.2009

Tatz, J. R., Soh, C., & Wessel, J. R. (2021). Common and unique inhibitory control signatures of action-stopping and attentional capture suggest that actions are stopped in two stages. *The journal*

of neuroscience, JN-RM-1105-21. https://doi.org/10.1523/jneurosci.1105-21.2021

Tazoe, T., Sakamoto, M., Nakajima, T., Endoh, T., Shiozawa, S., & Komiyama, T. (2009). Remote facilitation of supraspinal motor excitability depends on the level of effort. *European Journal of Neuroscience, 30*(7), 1297–1305. https://doi.org/10.1111/j.1460-9568.2009.06895.x

Verbruggen, F., Aron, A. R., Band, G. P., Beste, C., Bissett, P. G., Brockett, A. T., Brown, J. W., Chamberlain, S. R., Chambers, C. D., Colonius, H., Colzato, L. S., Corneil, B. D., Coxon, J. P., Dupuis, A., Eagle, D. M., Garavan, H., Greenhouse, I., Heathcote, A., Huster, R. J., & Boehler, C. N. (2019). A consensus guide to capturing the ability to inhibit actions and impulsive behaviors in the stop-signal task. *ELife, 8*, e46323. https://doi.org/10.7554/elife.46323

Volz, L. J., Hamada, M., Rothwell, J. C., & Grefkes, C. (2015). What makes the muscle twitch: Motor system connectivity and TMS-induced activity. *Cerebral Cortex, 25*(9), 2346–2353. https://doi.org/10.1093/cercor/bhu032

Wager, T. D., Sylvester, C.-Y. C., Lacey, S. C., Nee, D. E., Franklin, M., & Jonides, J. (2005). Common and unique components of response inhibition revealed by fMRI. *NeuroImage, 27*(2), 323–340. https://doi.org/10.1016/j.neuroimage.2005.01.054

Wagner, J., Wessel, J. R., Ghahremani, A., & Aron, A. R. (2018). Establishing a right frontal Beta signature for stopping action in scalp EEG: Implications for testing inhibitory control in other task contexts. *Journal of Cognitive Neuroscience, 30*(1), 107–118. https://doi.org/10.1162/jocn_a_01183

Wessel, J. R. (2020). β-Bursts reveal the trial-to-trial dynamics of movement initiation and cancellation. *The Journal of Neuroscience, 40*(2), 411–423. https://doi.org/10.1523/jneurosci.1887-19.2019

Wessel, J. R., & Aron, A. R. (2015). It's not too late: The onset of the frontocentral P3 indexes successful response inhibition in the stop-signal paradigm. *Psychophysiology, 52*(4), 472–480. https://doi.org/10.1111/psyp.12374

Wessel, J. R., & Aron, A. R. (2017). On the Globality of motor suppression: Unexpected events and their influence on behavior and cognition. *Neuron, 93*(2), 259–280. https://doi.org/10.1016/j.neuron.2016.12.013

Wessel, J. R., Diesburg, D. A., Chalkley, N. H., & Greenlee, J. D. W. (2022). A causal role for the human subthalamic nucleus in non-selective cortico-motor inhibition. *Current Biology, 32*(17), 3785–3791.e3. https://doi.org/10.1016/j.cub.2022.06.067

Wessel, J. R., Jenkinson, N., Brittain, J.-S., Voets, S. H. E. M., Aziz, T. Z., & Aron, A. R. (2016). Surprise disrupts cognition via a fronto-basal ganglia suppressive mechanism. *Nature Communications, 7*(1), 11195. https://doi.org/10.1038/ncomms11195

Wessel, J. R., Reynoso, H. S., & Aron, A. R. (2013). Saccade suppression exerts global effects on the motor system. *Journal of Neurophysiology, 110*(4), 883–890. https://doi.org/10.1152/jn.00229.2013

Wessel, J. R., Waller, D. A., & Greenlee, J. D. (2019). Non-selective inhibition of inappropriate motor-tendencies during response-conflict by a fronto-subthalamic mechanism. *ELife, 8*, e42959. https://doi.org/10.7554/elife.42959

Wilson, J. M., Thompson, C. K., McPherson, L. M., Zadikoff, C., Heckman, C. J., & MacKinnon, C. D. (2020). Motor unit discharge variability is increased in mild-to-moderate Parkinson's disease. *Frontiers in Neurology, 11*, 477. https://doi.org/10.3389/fneur.2020.00477

Witham, C. L., Riddle, C. N., Baker, M. R., & Baker, S. N. (2011). Contributions of descending and ascending pathways to corticomuscular coherence in humans. *The Journal of Physiology, 589*(15), 3789–3800. https://doi.org/10.1113/jphysiol.2011.211045

Zicher, B., Ibáñez, J., & Farina, D. (2022). Beta inputs to motor neurons do not directly contribute to volitional force modulation. *The Journal of Physiology*. https://doi.org/10.1113/jp283398

Authors and Affiliations

Benjamin O. Rangel[1,2,3] · Giacomo Novembre[4] · Jan R. Wessel[2,5,6]

✉ Benjamin O. Rangel
benjamin-rangel@uiowa.edu

[1] Interdisciplinary Graduate Program in Neuroscience, University of Iowa, Iowa City, IA 52245, USA

[2] Cognitive Control Collaborative, University of Iowa, Iowa City, IA 52245, USA

[3] University of Iowa, 444 Medical Research Center, Iowa City, IA 52242, USA

[4] Neuroscience of Perception & Action Laboratory, Italian Institute of Technology, Rome, Italy

[5] Department of Psychological and Brain Sciences, University of Iowa, Iowa City, IA 52245, USA

[6] Department of Neurology, University of Iowa Hospitals and Clinics, Iowa City, IA 52242, USA